Korean J. Chem. Eng., **31**(9), 1695-1706 (2014)
DOI: 10.1007/s11814-014-0099-y

pISSN: 0256-1115
eISSN: 1975-7220

The influences of collector diameter, spinneret rotational speed, voltage, and polymer concentration on the degree of nanofibers alignment generated by electrocentrifugal spinning method : Modeling and optimization by response surface methodology

Mehrdad Khamforoush*,†, Tayyebeh Asgari*, Tahmasb Hatami*, and Farzad Dabirian**

*Department of Chemical Engineering, Faculty of Engineering, University of Kurdistan, Sanandaj 66177, Iran
**Department of Mechanical Engineering, Faculty of Engineering, Razi University, Kermanshah 67149, Iran
(*Received 4 January 2014 • accepted 3 April 2014*)

Abstract−We studied the capability of electrocentrifuge-spinning (ECS) method for generating highly aligned nanofiber. First, the degree of nanofiber alignment (DNA) produced by ECS was compared with that of rotating drum (RD) method and ECS superiority was demonstrated. Then central composite design (CCD) and response surface methodology (RSM) was used for optimization of operating conditions. The critical factors selected for the examination were voltage, polymer concentration, collector diameter and spinneret rotational speed. To design the required experiments at the settings of independent parameters, RSM was applied. A total of 30 experiments were accomplished towards the construction of a quadratic model for target variable. Using this quadratic model, the influence of aforementioned variables was discussed on DNA. The best operating condition for attaining the maximum value of DNA was the applied voltage of 20.19 kV, polymer concentration of 17.44 wt%, collector diameter of 40.76 cm, and rotational speed of 2680.10 rpm.

Keywords: Electrocentrifuge-spinning, Highly Aligned Nanofiber, Response Surface Methodology, Optimization

INTRODUCTION

Electrospinning has attracted considerable attention due to its potential as a simple and versatile technology to produce polymer fibers [1-5]. In conventional electrospinning, electrospun fibers are deposited randomly in a non-woven arrangement on the grounded collector. This is mainly due to the formation and growth of whipping instability during stretching process of electrified polymeric jet [6,7]. Such non-woven electrospun nanofibers have limited applications as the adsorbent, filtration media, catalyst support, wound dressing, and tissue engineering scaffold [1]. This restricts the areas in which electrospun nanofibers can be exploited. To extend the usage of nanofibers for advanced applications such as implementation of small-scale electronic devices [8-10], cell maturation in neural tissue engineering [11-13], blood vessel engineering [14], and improving the tensile strength of nanofibers [15-17] only continuous well-aligned single nanofibers or uniaxial fiber bundles are applicable. However, due to the electrostatic interactions between external electric field and surface charges on jet, controlled fabrication of nanofibers is a major challenge in this field.

To date, several approaches have been suggested to produce uniaxial aligned nanofibers. In these methods, the collector of conventional electrospinning apparatus is replaced by a rotating drum [18, 19], a sharp-edge rotating disk [20], parallel conducting electrodes [21-23], a fin rotor [24], two charged copper disks [25], and a hollow cylinder [26]. Although fiber alignment has somewhat improved by these techniques, there are still several drawbacks for the purposes of practical applications of nanofibers. In the method of using RD as the collector, DNA is not so favorable [1,26]. The other methods produce aligned fibers with limited length [21-24] and over a narrow area [20]. Additionally, these methods have been restricted with low production rate of aligned nanofibers that is another major challenge in commercialization of aligned nanofibers production.

Recently, Dabirian et al. developed a simple high-performance technique named ECS [27,28] to generate polymeric nanofiber. In this technique, electrical and centrifugal forces are employed simultaneously to generate aligned nanofiber. Dabirian et al. [28] also studied the jet formation process in ECS by high-speed photography and proposed that this technique can be employed to generate bundles of aligned nanofiber.

In this investigation, by performing a minor change in the positioning of ECS setup developed by Dabirian et al. [27,28], we evaluated the capability of ECS to generate highly-aligned nanofiber. To assess the effectiveness of the modified device, DNA at various processing condition was compared with those obtained using a standard electrospinning technique such as RD method. Our results revealed that DNA in ECS method was on average more than three-times higher than the corresponding values in RD method.

It is usually essential for applicable engineering data to be modeled and analyzed for determining the conditions under which the highest process performance is attained. RSM [29] and other relevant experimental design techniques are well-known methods for this purpose that are used by many researchers especially in chemical engineering [5,30-32]. Therefore, another aim of this work was using RSM in conjunction with central composite design to establish the functional relationships between spinneret rotational speed, polymer concentration, collector diameter, and voltage with DNA. Then, this relationship was used for determining the optimal oper-

†To whom correspondence should be addressed.
E-mail: m.khamforoush@uok.ac.ir, m_khamforoush@yahoo.com

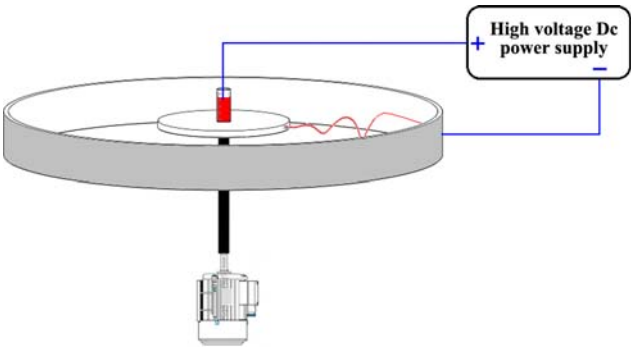

Fig. 1. ECS device for generating highly aligned nanofibers.

ating conditions to attain the highest value of DNA.

MATERIALS AND METHODS/EXPERIMENTAL

1. Materials

Industrial grade polyacrylonitrile (PAN) with a weight-average molecular weight of about 100000 g/mol was obtained from Polyacryle IRAN Company as the polymer and N, N-dimethylformamide (DMF) was purchased from Merck Company as the solvent. Polymer solution was prepared by dissolving PAN in DMF with the concentration of 14 to 19 wt%. Afterwards, it was kept in a constant temperature around 50 °C for 2 hours to complete the dissolution. The polymer solution was then placed in a special handmade container equipped with a flat-tipped stainless steel needle (0.5× 15 mm) as the spinneret. The needle was connected to the positive terminal of a high DC voltage power supply.

2. Experimental Apparatus and Procedure

2-1. ECS Setup

The ECS setup was detailed by Dabirian et al. [27] and is illustrated in Fig. 1. In two research efforts by Dabirian et al. [27,28], the setup was installed in vertical position. However in this study, the ECS setup was installed in horizontal position for production of highly aligned nanofiber. The experimental setup consists of a special handmade cylindrical container mounted horizontally on the center of a flat rotating disk. The container is equipped with a flat-tipped stainless steel needle as the spinneret. The collection of container and flat rotating disk is positioned horizontally at the center of a hollow cylindrical collector and is joined to a high speed three-phase electromotor with adjustable RPM. In this study, a syringe needle with diameter of 0.5 mm and length of 15 mm was used as the spinneret and a metallic hollow cylinder with 8 cm height has been used as collector. Once the container started to rotate and centrifugal force was applied, the polymer solution was drained out of the needle. The polymer solution was ejected from the tip of spinneret as soon as a potential difference greater than the critical voltage was applied between the spinneret and cylindrical fiber collector. The spinneret and fiber collector were connected to the positive and negative terminals of a high voltage DC power supply, respectively. Due to the high rotational speed of spinneret and exposing the outlet polymer solution to surrounding air, the ejected solution from the nozzle tip was immediately dried. Therefore, the polymer solution did not have enough time to reach the collector. Actually, the main drawback of ECS setup was the blocking of its nozzle by the dried polymer. To overcome this problem, the spinneret and container have been enclosed with a cylindrical cap in a way that only 2 mm of spinneret tip has remained uncovered.

2-2. RD Setup

In this study, a single RD has been employed to generate aligned fibers. The setup is comprised of a rotating drum with diameter of 5 cm that has been covered by a layer of aluminum foil to collect the fibers. A moving syringe pump with reciprocal movement along the cylinder axis is installed in front of the RD to feed the spinneret.

3. Experimental Design

In this paper, RSM was applied to model and optimize the ECS parameters for generating aligned nanofiber with maximum degree of orientation. Applying RSM especially for optimization problems has several advantages, like time and material saving and low operating costs [33]. RSM has four basic steps [34]. First, it specifies several experiments for measuring the dependent variable at various conditions. The user then performs the required experiments and measures the values of dependent variable. All the experiments should be carried out as near as possible to the recommended conditions by RSM. This minimizes the effect of experimental error in the observed response. Then, RSM develops a simple formula to correlate the dependent and independents variables. In most common problems, a second-order formula is suitable for this purpose [29,33,34]. By applying the developed formula, RSM then determines the best set of conditions to optimize the response. Finally, it depicts the influences of independent variables (factors) through two- and three-dimensional figures.

RESULTS AND DISCUSSION

1. Comparison between ECS and RD Methods

To compare the ability of ECS and RD methods for producing highly aligned nanofibers, both methods were evaluated at the same operating condition. The selected parameters that had direct effect on the DNA were voltage, polymer concentration, spinneret collector distance, RPM, and feed flow rate. As the feed flow rate of ECS method [27] is affected by both rotational speed of spinneret and applied voltage, first the polymer flow rate was measured at selected RPMs, namely, 1200 and 2000 for various voltages from 10 kV to 22 kV. Then, the corresponding values of feed flow rate in each RPM and voltage were set for the feed pump of RD method. The measured flow rates of polymer solution for ECS are depicted in Table 1. Other operating conditions were 17 wt% for polymer concentration, 14 cm for spinneret collector distance, and 10 kV to 22 kV for Voltage.

The degree of nanofiber alignment was determined using image analysis by Fourier transform analysis [35]. Nanofibers were deposited on a glass microscope slide or a transparent plastic film for a short time around of 20 sec. For each ECS and RD parameter, the

Table 1. Feed flow rate (ml/h) at various voltages and RPMs in ECS and RD methods

RPM \ Voltage	10 kV	13 kV	16 kV	19 kV	22 kV
1200	0.45	0.45	0.5	0.6	0.56
2000	0.7	0.73	0.74	0.81	0.87

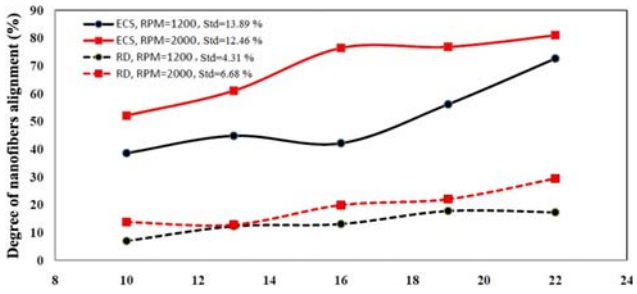

Fig. 2. Comparison between DNA in ECS and RD methods.

experiment was repeated thirty times and several optical images were captured from each sample with an optical microscope (BEL-BIO2). Finally, one-hundred images were chosen for alignment analysis, and the average value of nanofiber alignment of these images was reported as DNA. The variation of DNA against applied voltage for both ECS and RD methods is represented in Fig. 2. In addition, the values of standard deviation (Std) for each curve are depicted in this figure. The values of RPM in this figure were kept constant at 1200 and 2000. For comparison of the results, consider the values of DNA at 2000rpm and the voltages of 10 kV, 13 kV, 16 kV, 19 kV, and 22 kV. The numerical values for RD at these conditions were 13.7%, 12.76%, 19.8%, 21.95%, and 29.4%, respectively. However, the corresponding values for ECS were 52%, 61%, 76.4%, 76.8%, and 81%, respectively. These numerical values indicated that the DNA for ECS method was on average more than three-times as high as the RD method.

The morphology of fabricated aligned nanofibers was characterized via optical and scanning electron microscopy. The typical optical micrographs of PAN nanofibers by ECS and RD methods are depicted in Fig. 3. From this figure one can see that the type of electrospinning approach has a remarkable influence on the DNA. According to this figure, an obviously higher value of DNA was obtained for ECS method.

2. Statistical Analysis of the Experimental Data

Independent factors in the current study were voltage, polymer concentration, collector diameter, and spinneret rotational speed. The only dependent variable was DNA. Using Design Expert software, a 4-factor-5-level CCD was applied as the central composite design (CCD). Each independent variable was coded at five levels between $-\beta$ and $+\beta$. The variation domains of independent variables were 8-22 kV for voltage; 14-19 wt% for polymer concentration, 20-60 cm for collector diameter, and, 800-4,500 rpm for spinneret rotational speed. The levels of factors are shown in Table 2.

The form of proposed formula for calculating the DNA as functions of the four independent variables was as follow:

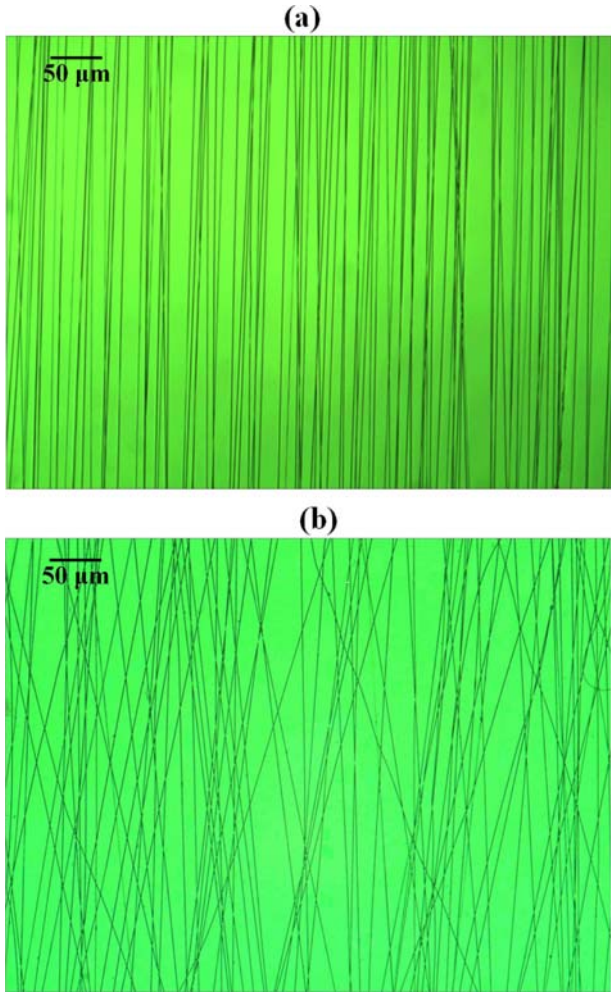

Fig. 3. The typical optical micrographs of PAN nanofibers by applied voltage of 22 kV and polymer concentration of 17 wt% for (a) ECS method with collector diameter of 40 cm and rotating speed of 2,000 rpm (b) RD method with the distance between drum and spinneret tip of 14 cm and rotating speed of 2,000 rpm.

$$DNA\% = \beta_0 + \beta_1 A + \beta_2 B + \beta_3 C + \beta_4 D + \beta_{12} AB + \beta_{13} AC + \beta_{14} AD + \beta_{23} BC + \beta_{24} BD + \beta_{34} CD + \beta_{11} A^2 + \beta_{22} B^2 + \beta_{33} C^2 + \beta_{44} D^2 \quad (1)$$

where β_0 is the formula constant; β_1, β_2, β_3 and β_4 are linear coefficients; β_{12}, β_{13}, β_{14}, β_{23}, β_{24} and β_{34} are cross product coefficients, and β_{11}, β_{22}, β_{33} and β_{44} are the quadratic coefficients [36]. The param-

Table 2. The levels of factors in the ECS experiments based on central composite design (CCD)

Factor	Coded levels of variables				
	Low axial	Low factorial	Center	High factorial	High axial
	$(-\beta)$	(−1)	(0)	(+1)	$(+\beta)$
A: Voltage (kV)	8	11.5	15	18.5	22
B: Concentration (wt%)	14	15.25	16.5	17.75	19
C: Diameter (cm)	20	30	40	50	60
D: Rotational speed (rpm)	800	1725	2650	3575	4500

eters A, B, C, and D in this formula refer to the coded values of voltage, polymer concentration, collector diameter, and spinneret rotational speed, respectively. Expert Design software determines the values of these constants in order that minimizes the deviation of this formula from the experimental data.

As the number of experiments at the design center was suggested to be six [37], the total number of experiments must be equal to $2^k+(2\times k)+6=30$ [38], where k is the number of independent factors. After specifying the required experiments, the values of independent variables were coded to lie at ±1, 0, and ±β. The actual values of independent variables for these 30 unique experiments together with their corresponding coded level are shown in Table 3.

As soon as the requested DNA data were obtained from the experiments, the unknown coefficients of Eq. (1) were calculated by applying least squares method. The relationship between DNA and coded variables is presented in the following equation:

$$\begin{aligned}\text{DNA\%}=&69.52+13.36A+6.88B-6.24C-2.9D\\&+3.05AB+11.33AC+0.44AD-3.37BC+2.64BD-3.23CD\\&-4.02A^2-3.47B^2-9.17C^2-10.15D^2\end{aligned} \quad (2)$$

The analysis of variance (ANOVA) for the response is summarized in Table 4. The value of 43.46 obtained for Model F-value indirectly suggested that the proposed formula for calculating DNA% was significant. The possibility that such large value of F-value could occur as a result of noise is only 0.01%. The p-value parameter in this table determines whether the model terms of A, B, C, D, AB, AC, AD, BC, BD, CD, A^2, B^2, C^2, and D^2 are important or not. The parameters with the p-value more than 0.0500 did not have significant effect on the response. So for the current case, the entire model terms with the exception of AD were significant. Referring to Table 4, the R^2 value was about 0.9759. The relatively high value of R^2 indicated that the proposed quadratic equation was capable of accurately predicting DNA. Due to the five level independent variables, the model equation in our case includes additional terms. Therefore, adjusted R^2 parameter (Adj-R^2) for the degrees of freedom was chosen to be examined as well. Adj-R^2 is much less sensitive to the degrees of freedom than R^2 and does not affect seriously by adding

Table 3. The experimental design for the four independent variables and response at different factor levels

Run	Factors				Response
	Voltage (kV)	Concentration (wt%)	Diameter (cm)	Rotational speed (rpm)	Degree of nanofiber alignment (%)
1	11.5(−1)[a]	15.25(−1)[a]	50(+1)[a]	1725(−1)[a]	25.00
2	22.0(+β)	16.50(0)	40(0)	2650(0)	83.00
3	15.0(0)	16.50(0)	40(0)	2650(0)	68.00
4	15.0(0)	19.00(+β)	40(0)	2650(0)	73.00
5	15.0(0)	16.50(0)	40(0)	4500(+β)	18.56
6	18.5(+1)	15.25(−1)	50(+1)	1725(−1)	63.00
7	15.0(0)	16.50(0)	40(0)	2650(0)	71.00
8	11.5(−1)	15.25(−1)	30(−1)	1725(−1)	39.00
9	11.5(−1)	15.25(−1)	50(+1)	3575(+1)	8.00
10	15.0(0)	16.50(0)	40(0)	2650(0)	70.45
11	18.5(+1)	15.25(−1)	30(−1)	1725(−1)	40.00
12	11.5(−1)	15.25(−1)	30(−1)	3575(+1)	39.00
13	18.5(+1)	15.25(−1)	30(−1)	3575(+1)	40.00
14	11.5(−1)	17.75(+1)	30(−1)	1725(−1)	54.53
15	15.0(0)	16.50(0)	40(0)	2650(0)	75.00
16	11.5(−1)	17.75(+1)	50(+1)	3575(+1)	8.09
17	15.0(0)	16.50(0)	40(0)	800(−β)	38.00
18	15.0(0)	16.50(0)	60(+β)	2650(0)	17.46
19	15.0(0)	14.00(−β)	40(0)	2650(0)	37.00
20	18.5(+1)	15.25(−1)	50(+1)	3575(+1)	43.58
21	18.5(+1)	17.75(+1)	50(+1)	3575(+1)	69.14
22	15.0(0)	16.50(0)	40(0)	2650(0)	66.91
23	11.5(−1)	17.75(+1)	30(−1)	3575(+1)	57.60
24	8.0(−β)	16.50(0)	40(0)	2650(0)	22.65
25	15.0(0)	16.50(0)	20(−β)	2650(0)	47.00
26	11.5(−1)	17.75(+1)	50(+1)	1725(−1)	13.00
27	18.5(+1)	17.75(+1)	50(+1)	1725(−1)	69.00
28	18.5(+1)	17.75(+1)	30(−1)	3575(+1)	63.45
29	18.5(+1)	17.75(+1)	30(−1)	1725(−1)	56.00
30	15.0(0)	16.50(0)	40(0)	2650(0)	65.79

[a]Level code values of the parameters

Table 4. Analysis of variance for response surface quadratic model

Source	Sum of squares	df	Mean square	F value	p-value prob>F
Model	13815.97	14	986.85	43.46	<0.0001
A-V	4284.02	1	4284.02	188.66	<0.0001
B-PC	1137.54	1	1137.54	50.10	<0.0001
C-CD	935.63	1	935.63	41.20	<0.0001
D-RPM	201.55	1	201.55	8.88	0.0094
AB	148.78	1	148.78	6.55	0.0218
AC	2054.58	1	2054.58	90.48	<0.0001
AD	3.07	1	3.07	0.14	0.7182
BC	181.78	1	181.78	8.01	0.0127
BD	111.14	1	111.14	4.89	0.0429
CD	167.12	1	167.12	7.36	0.0160
A^2	442.84	1	442.84	19.50	0.0005
B^2	331.09	1	331.09	14.58	0.0017
C^2	2304.86	1	2304.86	101.50	< 0.0001
D^2	2828.18	1	2828.18	124.55	< 0.0001
R^2	0.9759				
Adj R^2	0.9535				
Pred R^2	0.8785				
Adeq precision	23.17				

further terms to the model. Therefore, it is a better criterion for determination the goodness of fit. According to Table 4, the Adj-R^2 value for the response was 0.9535. The Pred R^2 of 0.8785 was in reasonable agreement with the value of Adj R^2. The term "Adeq Precision" in the last row of this table indicates the signal to noise ratio. For a desirable model, this ratio should be greater than 4. Of course, the level of significance of the operating parameters was investigated in this study only for PAN in DMF solution and their effects may not be reliable for other polymers.

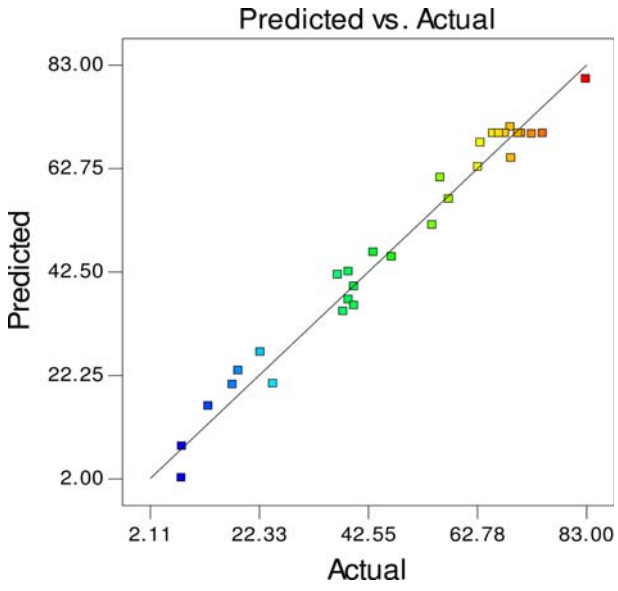

Fig. 4. The scatter plot of predicted DNA by equation (2) versus the corresponding experimental data.

To clarify the goodness of the proposed model, Fig. 4 shows the scatter plot of experimental data with those obtained from Eq. (2). The points marked by filled squares are concentrated near the diagonal line. This obviously indicates that Eq. (2) predicts the experimental data reasonably well.

3. Characterization of Fabricated Nanofibers by ECS Method

Six optical images of nanofibers obtained by ECS method along with their corresponding normalized angular power spectrum (APS)s are depicted in Fig. 5. These images were obtained at the applied voltages of 8, 15, and 22 kV, rotational speed of 800 and 2,650 rpm, collector diameters of 20 and 40 cm, and polymer concentrations of 14, 16.5, and 19%. According to these graphs, random fibers structures were obtained for the experiments, including any of the following operating conditions: the rotational speed of 800 rmp, polymer concentration of 14 wt%, and applied voltage of 8 kV. The micrographs clearly show that for the operating conditions for the cases (c) (the collector diameter of 40 cm, rotational speed of 2,650 rpm, voltage of 15 kv, and polymer concentration of 19%) and (e) (the collector diameter of 40 cm, rotational speed of 2,650 rpm, voltage of 22 kV, and polymer concentration of 16.5 wt%), there was a high degree of parallelism among nanofibers. This later result can be also demonstrated by investigating the APSs graphs. In Fig. 5, the peaks of APSs for cases (c) and (e) are sharper than the others. Note that the sharper the peaks of APS, the higher the DNA will be.

Two typical SEM photographs of nanofibers mat, which were produced using ECS method, together with their corresponding diameter distributions are shown in Fig. 6. These pictures were obtained by applying two potential differences of 20 and 22 kV at the polymer concentration of 16.5 wt%, collector diameter of 40 cm, and rotating rate of 2,650 rpm. Mean, standard deviation, and the range of fiber diameters were determined in these SEM pictures. As can be seen, fibers in both pictures were oriented with high degree of alignment. The other point is that the average fiber diameter for the case of 20 kV potential differences (763.93 nm with the standard deviation of 47.66 nm) was lower than that of 22 kV (812.96 nm with the standard deviation of 39.25 nm). It clearly indicates that increasing the applied voltage increased the fiber diameters. Although the effect of potential difference on the fiber diameter is not completely investigated in this paper, it is well described in literature with more details. Actually, the influence of applied voltage on fiber diameter is not very clear. By increasing the voltage, electrostatic force on the polymer jet increases and it may reduce the fiber diameter. In general, by increasing the voltage, fiber diameter may be increased [39,40], decreased [2], or even unchanged [41]. In addition to the influence of voltage on the fiber diameter, it can lead to the production of a mixture of beads and fibers [40,42].

4. Sensitivity Analyses

As the accuracy of Eq. (2) for predicting the values of DNA well demonstrated, this equation was applied for calculating the DNA at various values of collector diameter, rotational speed, voltage, and polymer concentration. The variation trends of DNA with respect to these four parameters are given in Fig. 7. To clarify the results, each three-dimensional graph is also shown in two-dimensional view in the left hand side. In each figure, while two of these four independent parameters were kept constant, the influences of the other parameters on the DNA were examined. The parameters V, PC, CD, and SRS in these figures refer to voltage, polymer concentration, col-

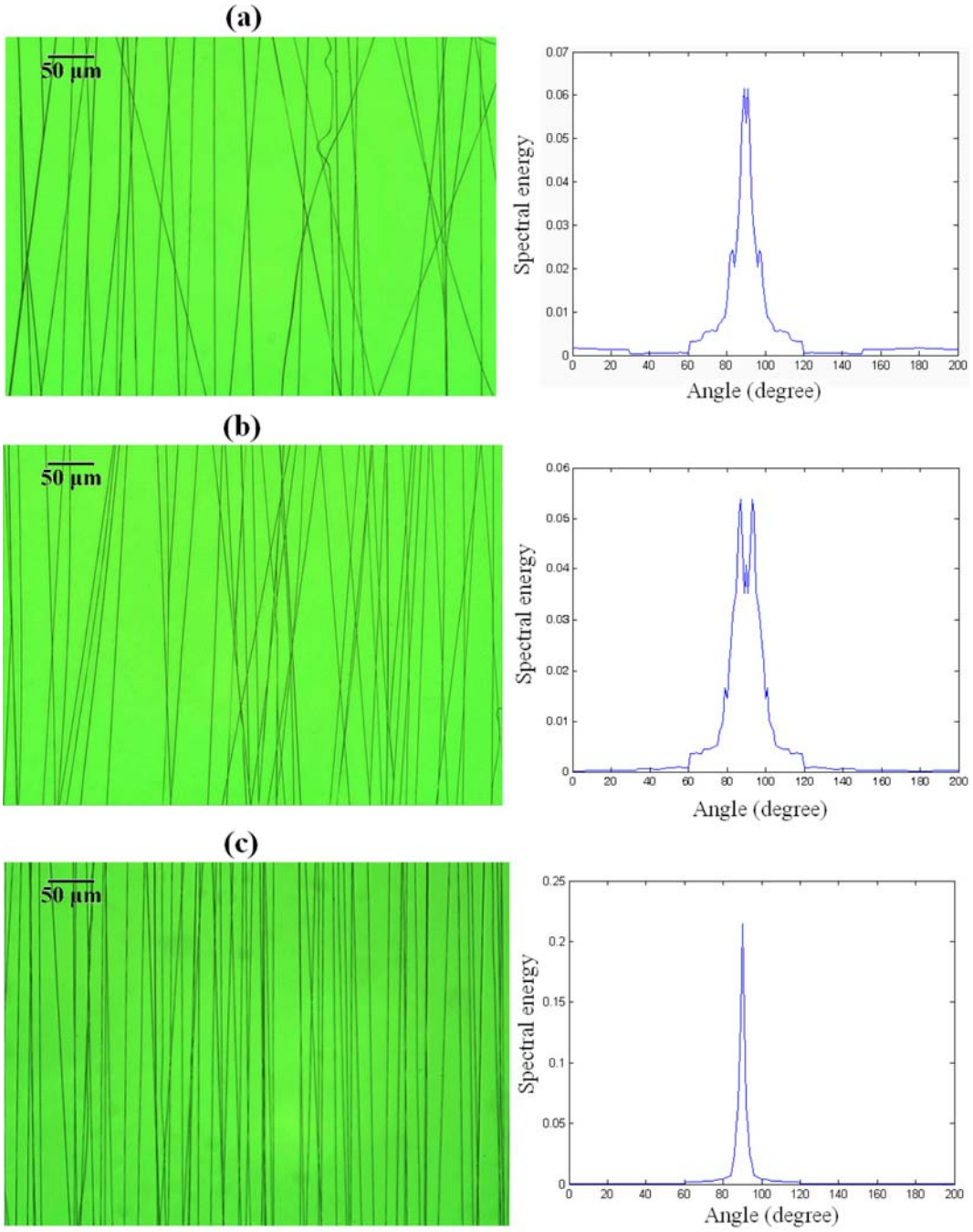

Fig. 5. Optical micrographs of aligned PAN nanofibers with corresponding normalized APSs generated by ECS method, respectively, at collector diameter, rotational speed, voltage, and polymer concentration of (a) 40 cm, 2,650 rpm, 8 kV, and 16.5 wt% (b) 40 cm, 2,650 rpm, 15 kV, and 14 wt% (c) 40 cm, 2,650 rpm, 15 kV, and 19 wt% (d) 20 cm, 2,650 rpm, 15 kV, and 16.5 wt% (e) 40 cm, 2,650 rpm, 22 kV, and 16.5 wt% (f) 40 cm, 800 rpm, 15 kV, and 16.5 wt%.

lector diameter, and spinneret rotational speed, respectively. According to these figures, the influences of the four independent parameters were investigated item by item in the following subsections.

4-1. The Effect of Voltage on DNA

Fig. 7(a) shows the dependency of DNA by applied voltage and polymer concentration at a constant rotational speed and collector diameter of 2,650 rpm and 40 cm, respectively. It is inferred from this figure that for each arbitrary polymer concentration, the DNA increased constantly with increasing voltage. In accord with the two-dimensional graph depicted in Fig. 7(a), the DNA at 11.5 kv and the polymer concentration of 17.1% was close to 53.8%, while the corresponding value at 15 kv and the same concentration was approximately 71.8%. It means that increasing the voltage intensified the electrostatic field, and it in turn enhanced the DNA. The effect of voltage on DNA for various collector diameters is shown in Fig. 7(b). Based on this figure, the voltage effect was more significant at higher collector diameter. To complete the investigation of voltage effect on DNA, Fig. 7(c) represents its effect for a specified range

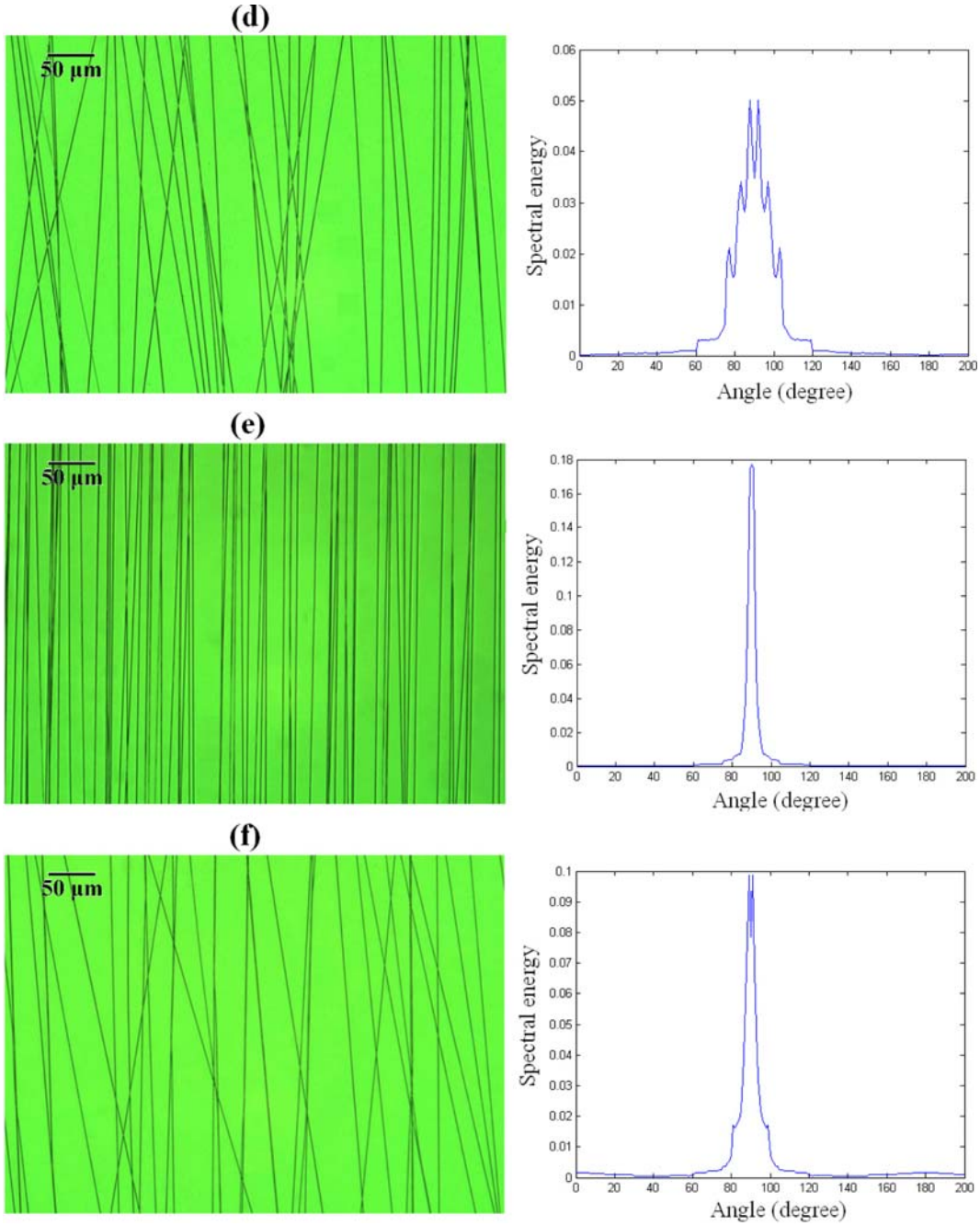

Fig. 5. Continued.

of spinning rotational speed. As shown by this figure, the DNA, for the entire domain of rotational speed, increased with applied voltage.

4-2. The Effect of Polymer Concentration on DNA

To fabricate uniform thin fibers, the polymer concentration has an inevitable degree of importance. With low concentration of polymer solution, not only there is always the possibility of bead formation but also no continuous fiber is produced. On the other side, polymer with higher concentration causes higher solution viscosity that consequently leads to the difficult ejection of jets and the formation of large diameter fibers [2,42-47]. In general, the change domain of polymer concentration should be in order to prevent the formation of beads or fibers with large diameter.

Similar to applied voltage, the effects of polymer concentration in combination with other three factors are depicted in Figs. 7(a), 7(d), and 7(e). The trend of these figures reveals that low polymer concentration caused the formation of disordered fibers in the collector surface. However, by increasing the polymer concentration, the value of DNA increased gradually. It can be also inferred from Fig. 7(a) that the effect of polymer concentration on fiber alignment was not as significant as voltage.

4-3. The Effect of Spinneret Rotational Speed on DNA

The effects of spinneret rotational speed on DNA are depicted in Figs. 7(c), 7(e), and 7(f). On the basis of these figures, by increasing

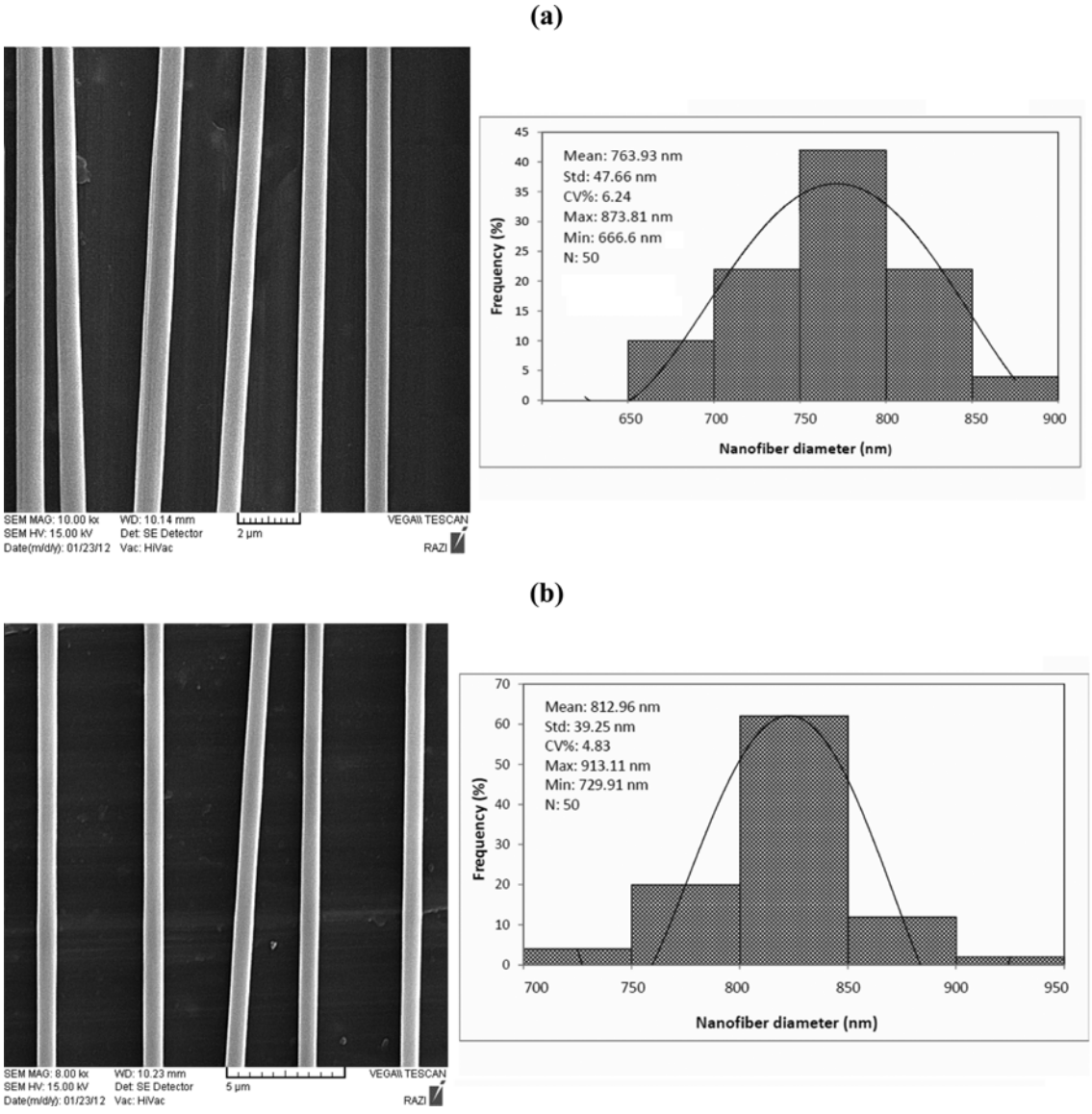

Fig. 6. SEM pictures of well-aligned PAN nanofibers produced by ECS method, respectively, at collector diameter, rotational speed, voltage, and polymer concentration of (a) 40 cm, 2,650 rpm, 20 kV, and 16.5 wt% (b) 40 cm, 2,650 rpm, 22 kV, and 16.5 wt%.

the spinneret rotational speed, the parallel percentage first increased and then decreased gradually. This phenomenon may have been due to the fact that increasing the rotational speed of spinneret to a certain extent increased the applied centrifugal force to the launched jet. Therefore, bending instability repulsive force disappeared from the collecting charges and a jet with greater stability was produced. At higher rotational speed, the irregular increasing of centrifugal force may have overcome on the surface tension force of polymer solution. This consequently ruptured launched polymer jets, and provided jets with turbulent movement. Therefore, a high speed rotating spinneret may have impacted the surrounding air and disrupted the air between the tip of the spinneret and collector and created vortices. This may have lost the stability of launched jet and reduced the value of DNA.

Determining the contribution of electrostatic and centrifugal forces on DNA is interesting. This is exactly similar to determining the contribution of voltage and spinneret rotational speed, respectively. Referring to Fig. 7(c), although both of these operating parameters influence the nanofiber orientation, the DNA is obviously more sensitive to voltage than SRS. Thus, the tremendous increasing of DNA in ECS is mainly due to the increasing of electrostatic forces.

4-4. The Effect of Collector Diameter on DNA

For investigating the effect of collector diameter on DNA, experiments were accomplished with the collector diameter range from 20 to 60 cm. The obtained results by RSM are shown in Figs. 7(b), 7(d), and 7(f). These figures indicated that DNA was an ascending-descending function of collector diameter. Furthermore, the effect of this parameter was to some extent similar to the effect of spinneret rotational speed. To justify the effect of collector diameter on the DNA it is worthwhile noting that at small values of collector diameter, the ejected solution from the nozzle tip was still wet by the time of reaching the collector. On the other side, at large values of collector diameter, some parts of polymer jets were unable to arrive at the collector surface and spread in the ECS chamber [27].

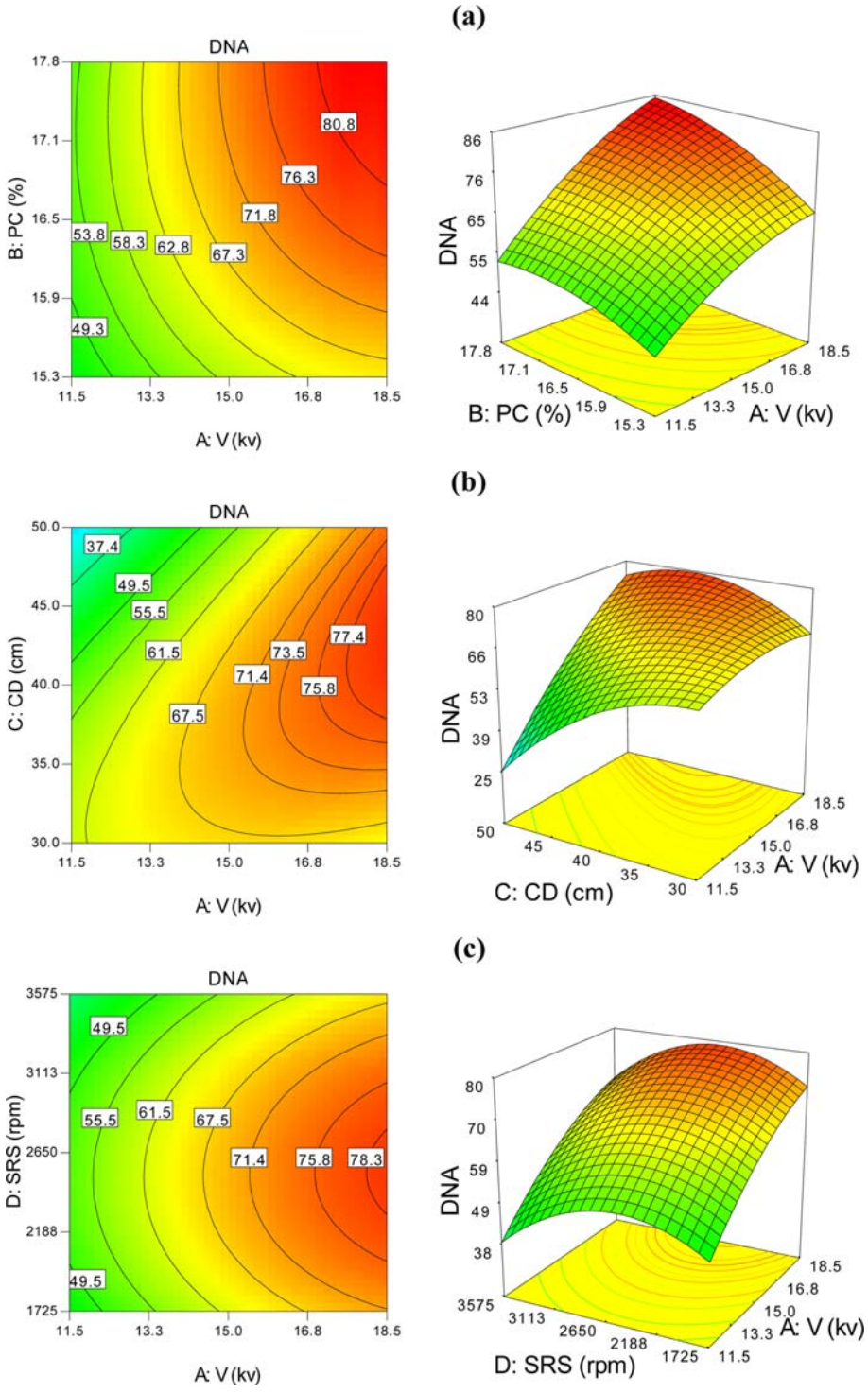

Fig. 7. The DNA dependency of (a) applied voltage and polymer concentration (b) applied voltage and collector diameter (c) applied voltage and spinneret rotational speed (d) polymer concentration and collector diameter (e) polymer concentration and spinneret rotational speed (f) collector diameter and spinneret rotational speed (In each graph, two of the parameters were kept constant at collector diameter of 40 cm, spinneret rotational speed of 2,650 rpm, polymer concentration of 16.5%, and applied voltage of 15 kV).

Therefore, the small values of DNA in the boundaries of these figures are completely logical. Accordingly, the collector diameter should be selected in a suitable range for producing aligned nanofibers.

5. Optimization

As mentioned, Expert Design software can determine the optimum values of independent variables to reach the highest amount of objective function, namely DNA. The results of optimization by this software are presented in Table 5. According to this table, the optimum values of independent variables were the applied voltage of 20.19 kV, polymer concentration of 17.44 wt%, collector diam-

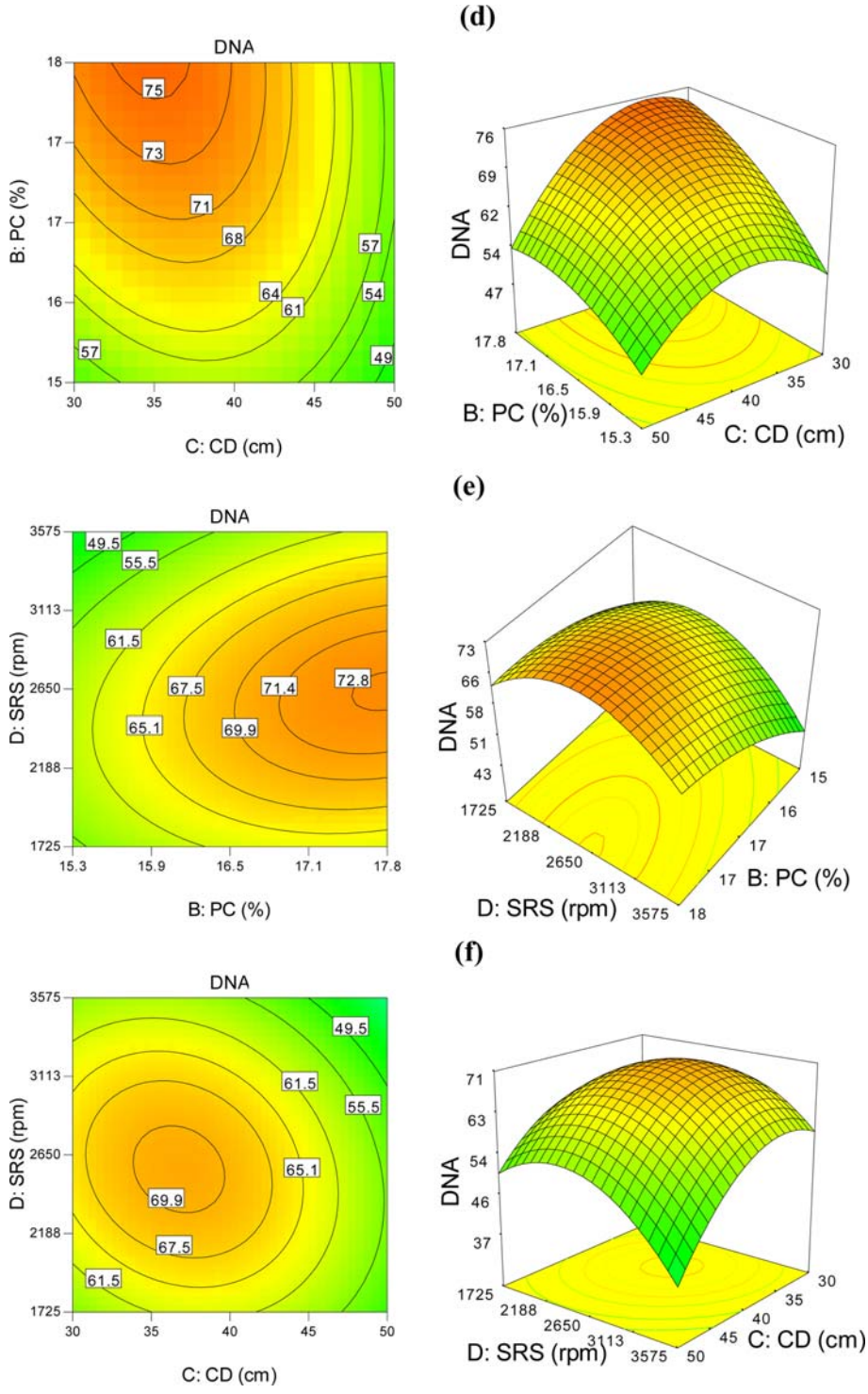

Fig. 7. Continued.

eter of 40.76 cm, and rotational speed of 2,680.10 rpm. The software predicted the value of 87.64% for DNA at this optimum condition. To check the accuracy of the predicted response at the 95% confidence interval of the optimum conditions, the ECS setup was operated accordingly. Table 5 presents the results of experiment conducted at the optimum condition and shows that the verification experiment and the predicted value from fitted correlations were in close agreement at a 95% confidence interval. These results revealed that the electrocentrifuge spinning can be efficiently employed to produce highly aligned nanofibers with several meters in length.

CONCLUSION

The production of aligned nanofibers using ECS method was investigated. The effect of four important parameters including collector diameter, applied voltage, spinning rotational speed, and poly-

Table 5. Verification experiment at the optimum conditions (spinneret rotational speed=2,680.10 rpm, polymer concentration=17.44 wt%, collector diameter=40.76 cm, and voltage=20.19 kV)

Response	Target	Correlation predicted	Confirmation experiment	Confidence interval (95%)	
				Low	High
DNA (%)	Maximize	87.64%	85.90%	80.84	94.43

mer concentration was investigated on the DNA. Expert Design software suggested a total of 30 unique experiments for a complete evaluation. Then, the required experiments were performed using an ECS setup. The main conclusions are as follows:

1) In agreement with the previous publications, ESC proved to be an efficient method for fabrication of highly aligned nanofibers.

2) Comparing the performance of ECS with RD method showed that the DNA of ECS method was at least three times more than that of RD method.

3) The experimental data of DNA as functions of the four operating parameters were well fitted by a second-order polynomial correlation.

4) From the four independent parameters under consideration, the applied voltage had the highest degree of influence on the DNA. Polymer solution concentration followed by collector diameter and spinning rotational speed also had significant effect on the morphology of generating fibers.

5) By applying either higher voltage or higher polymer weight fraction, the nanofibers were collected in more uniaxial lines.

6) The influence of collector diameter and spinning rotational speed was a little complicated. As each of these two factors increased, the DNA first increased and then decreased gradually.

7) Using RSM results, the maximum DNA was obtained with the applied voltage of 20.19 kV, polymer concentration of 17.44 wt%, collector diameter of 40.76 cm, and rotational speed of 2680.10 rpm. At this optimum condition, the predicted value of DNA by Expert Design software, 87.64%, was very close to its measuring value, 85.90%.

NOMENCLATURE

A : coded values of voltage
B : coded values of polymer concentration
C : coded values of collector diameter
CD : collector diameter [cm]
D : coded values of spinneret rotational speed
DNA : degree of nanofibers alignment [%]
PC : polymer concentration [wt%]
k : the number of independent factors
SRS : spinneret rotational speed [rpm]
V : voltage [kV]
β : constant

REFERENCES

1. Z. M. Huang, Y. Z. Zhang, M. Kotaki and S. Ramakrishna, *Compos. Sci. Technol*., **63**, 2223 (2003).
2. N. Bhardwaj and S. C. Kundu, *Biotechnol. Adv*., **28**, 325 (2010).
3. V. Mottaghitalab and A. K. Haghi, *Korean J. Chem. Eng*., **28**(1), 114 (2011).
4. M. Ziabari, V. Mottaghitalab and A. K. Haghi, *Korean J. Chem. Eng*., **25**(4), 923 (2008).
5. M. Kanafchian, M. Valizadeh and A. K. Haghi, *Korean J. Chem. Eng*., **28**(2), 428 (2011).
6. D. H. Reneker, A. L. Yarin, H. Fong and S. Koombhongse, *J. Appl. Phys*., **87**, 4531 (2000).
7. A. L. Yarin, S. Koombhongse and D. H. Reneker, *J. Appl. Phys*., **89**, 3018 (2001).
8. H. Wu, D. Lin, R. Zhang and W. Pan, *J. Am. Ceram. Soc*., **91**, 656 (2008).
9. C. Pan, H. Wu, C. Wang, B. Wang, L. Zhang, Z. Cheng, P. Hu, W. Pan, Z. Zhou, X. Yang and J. Zhu, *Adv. Mater*., **20**, 1644 (2008).
10. X. Lu, W. Zhang, C. Wang, T. C. Wen and Y. Wei, *Prog. Polym. Sci*., **36**, 671 (2011).
11. S. Y. Chew, R. Mi, A. Hoke and K. W. Leong, *Biomaterials*, **29**, 653 (2008).
12. S. H. Lim, X. Y. Liu, H. Song, K. J. Yarema and H. Q. Mao, *Biomaterials*, **28**, 1967 (2007).
13. B. S. Jha, R. J. Colello, J. R. Bowman, S. A. Sell, K. D. Lee, J. W. Bigbee, G. L. Bowlin, W. N. Chow, B. E. Mathern and D. G. Simpson, *Acta Biomater*., **7**, 203 (2011).
14. C. Y. Xu, R. Inai, M. Kotaki, S. Ramakrishna, *Biomaterials*, **25**, 877 (2004).
15. S. Y. Gu, Q. L. Wu, J. Ren and G. J. Vancso, *Macromol. Rapid Commun*., **26**, 716 (2005).
16. X. Wang, K. Zhang, M. Zhu, B. S. Hsiao and B. Chu, *Macromol. Rapid Commun*., **29**, 826 (2008).
17. G. Mathew, J. P. Hong, J. M. Rhee, D. J. Leo and C. Nah, *J. Appl. Polym. Sci*., **101**, 2017 (2006).
18. J. A. Matthews, G. E. Wnek, D. G. Simpson and G. L. Bowlin, *Biomacromolecules*, **3**, 232 (2002).
19. E. D. Boland, G. E. Wnek, D. G. Simpson, K. J. Palowski and G. L. Bowlin, *J. Macromol. Sci., Pure Appl. Chem. A*, **38**, 1231 (2001).
20. A. Theron, E. Zussman and A. L. Yarin, *Nanotechnology*, **12**, 384 (2001).
21. D. Li, Y. Wang and Y. Xia, *Nano Lett*., **3**, 1167 (2003).
22. R. Jalili, M. Morshed and S. A. Hosseini-Ravandi, *J. Appl. Polym. Sci*., **101**, 4350 (2006).
23. R. Jalili, S. A. Hosseini-Ravandi and M. Morshed, *Iranian J. Polym. Sci. Technol*., **4**, 241 (2006).
24. A. M. Afifi, H. Nakajima, H. Yamane, Y. Kimura and S. Nakano, *Macromol. Mater. Eng*., **294**, 658 (2009).
25. M. B. Bazbouz and G. K. Stylios, *J. Appl. Polym. Sci*., **107**, 3023 (2008).
26. L. S. Carnell, E. J. Siochi, N. M. Holloway, R. M. Stephens, C. Rhim, L. E. Niklason and R. L. Clark, *Macromolecules*, **41**, 5345 (2008).
27. F. Dabirian, S. A. H. Ravandi and A. R. Pishevar, *Curr. Nanosci*.,

6, 545 (2010).
28. F. Dabirian, S. A. H. Ravandi, A. R. Pishevar and R. A. Abuzade, *J. Electrostat*., **69**, 540 (2011).
29. J. Kwak, *Int. J. Mach. Tool Manuf*., **45**, 327 (2005).
30. D. Kim, Y. Song and Y. Park, *Korean J. Chem. Eng*., **30**(3), 664 (2013).
31. M. Ziabari, V. Mottaghitalab and A. K. Haghi, *Korean J. Chem. Eng*., **27**(1), 340 (2010).
32. B. Rahmanian, M. Pakizeh and A. Maskooki, *Korean J. Chem. Eng*., **29**(6), 804 (2012).
33. M. Kincl, S. Turk and F. Vrecer, *Int. J. Pharm*., **291**, 39 (2005).
34. V. Gunaraj, N. Murugan, *J. Mater. Process. Technol*., **88**, 266 (1999).
35. S. A. Hosseini Ravandi and K. Toriumi, *Text. Res. J*., **65**, 676 (1995).
36. D. C. Montgomery, *Design and analysis of experiments*, 6th Ed., Wiley, Singapore (2001).
37. G. E. P. Box and J. S. Hunter, *Ann. Math. Stat*., **28**, 195 (1957).
38. D. Obeng, S. Morrell and T. Napier, *Int. J. Miner. Process*., **769**, 181 (2005).
39. C. Zhang, X. Yuan, L. Wu, Y. Han and J. Sheng, *Eur. Polym. J*., **41**, 423 (2005).
40. M. Demir, I. Yilgor, E. Yilgor and B. Erman, *Polymer*, **43**, 3303 (2002).
41. D. Reneker and L. Chun, *Nanotechnology*, **7**, 216 (1996).
42. A. Haghi and M. Akbari, *Phys. Status. Solidi*., **204**, 1830 (2007).
43. C. Ki, D. Baek, K. Gang, K. Lee, I. Um and Y. Park, *Polymer*, **46**, 5094 (2005).
44. J. Deitzel, J. Kleinmeyer, D. Harris and N. Tan, *Polymer*, **42**, 261 (2001).
45. H. Liu and Y. Hsieh, *J. Polym. Sci. B-Polym. Phys*., **40**, 2119 (2002).
46. M. Mckee, G. Wilkes, R. Colby and T. Long, *Macromolecules*, **37**, 1760 (2004).
47. Y. Ryu, H. Kim, K. Lee, H. Park and D. Lee, *Eur. Polym. J*., **39**, 1883 (2003).